Supporting Information for

High performance organic photorefractive materials comprising 2-ethylhexyl plasticized poly(triarylamine)

Kuo-Lung Wang,[a, b] Jia-Cheng Jiang,[b] Cang-He Jhu,[b] Satoshi Wada,[a]
Takafumi Sassa*[a] and Masaki Horie*[b]

[a] Photonics Control Technology Team, RIKEN Center for Advanced Photonics, 2-1 Hirosawa, Wako, Saitama 351-0198, Japan. Email: tsassa@riken.jp

[b] Department of Chemical Engineering, National Tsing-Hua University, 101, Section 2, Kuang-Fu Road, Hsinchu, 30013 Taiwan. E-mail: mhorie@mx.nthu.edu.tw

Contents

1. Characterization of polymers

1.1 MALDI-TOF mass spectra

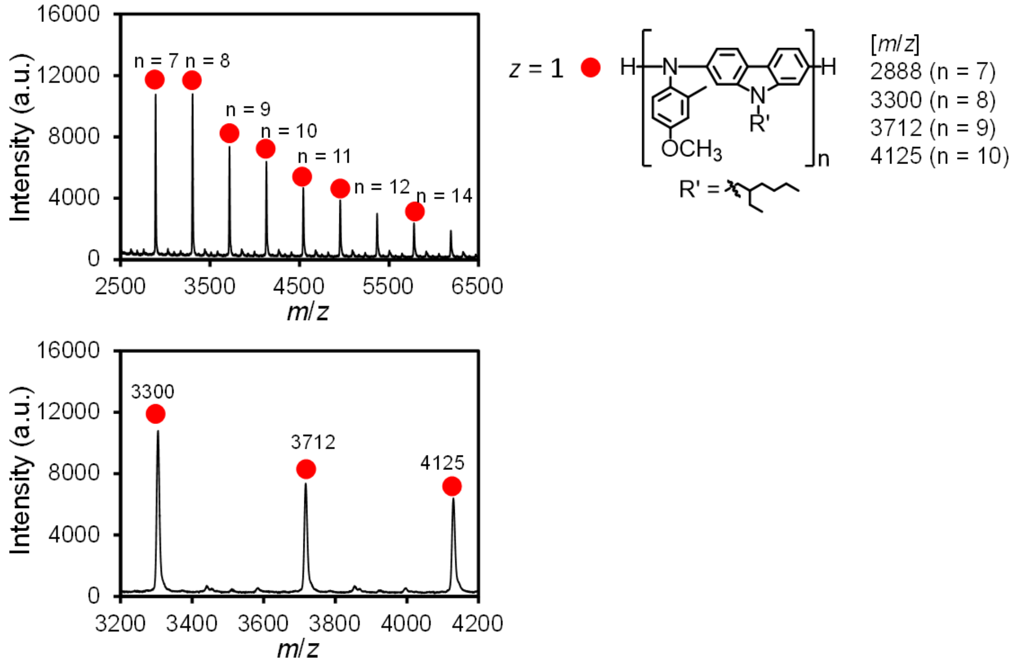

Fig. S1 MALDI-TOF mass spectrum of **P1**.

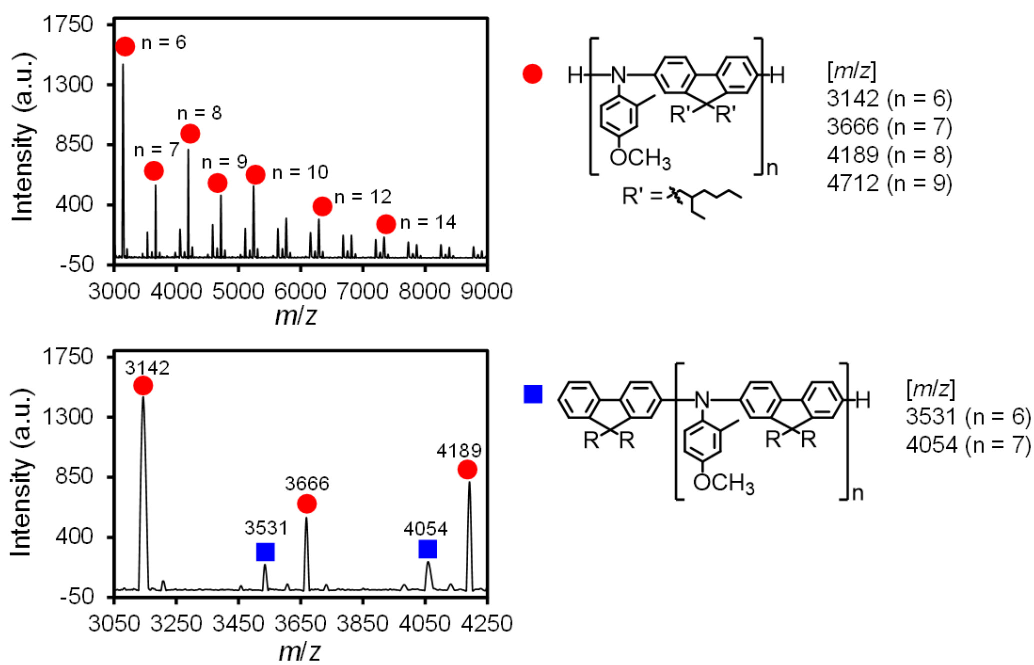

Fig. S2 MALDI-TOF mass spectrum of **P3**.

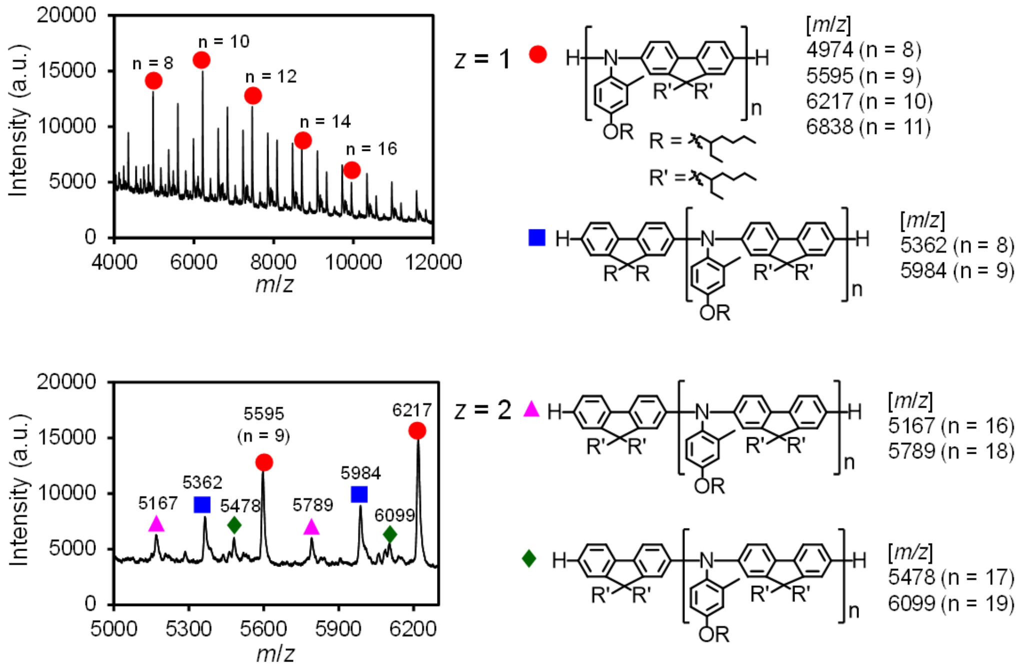

Fig. S3 MALDI-TOF mass spectrum of **P4**.

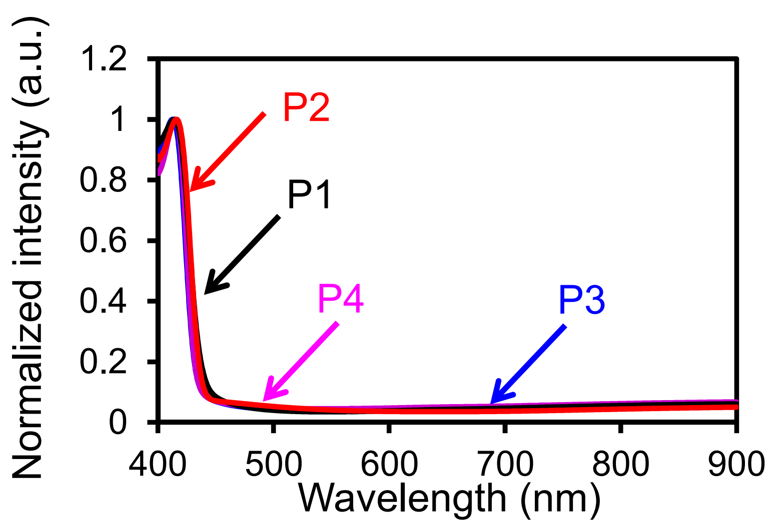

Fig. S4 UV-Vis spectra of thin film of **P1**, **P2**, **P3** and **P4**.

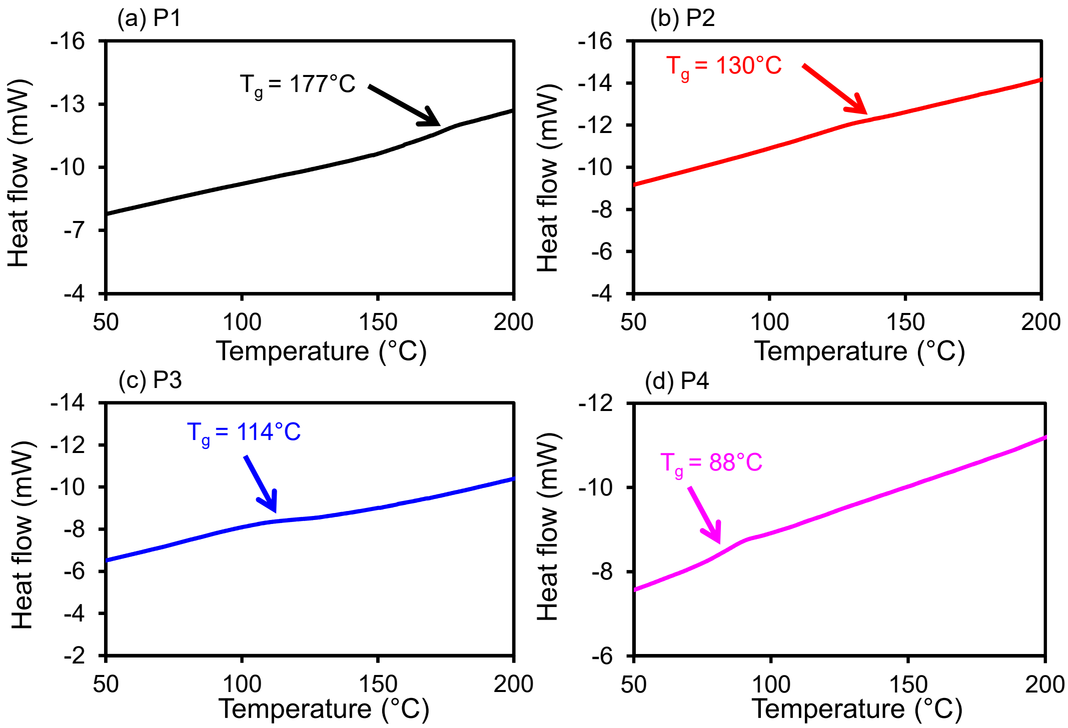

Fig. S5 DSC curves of **P1**, **P2**, **P3** and **P4**.

2. OFET characteristics

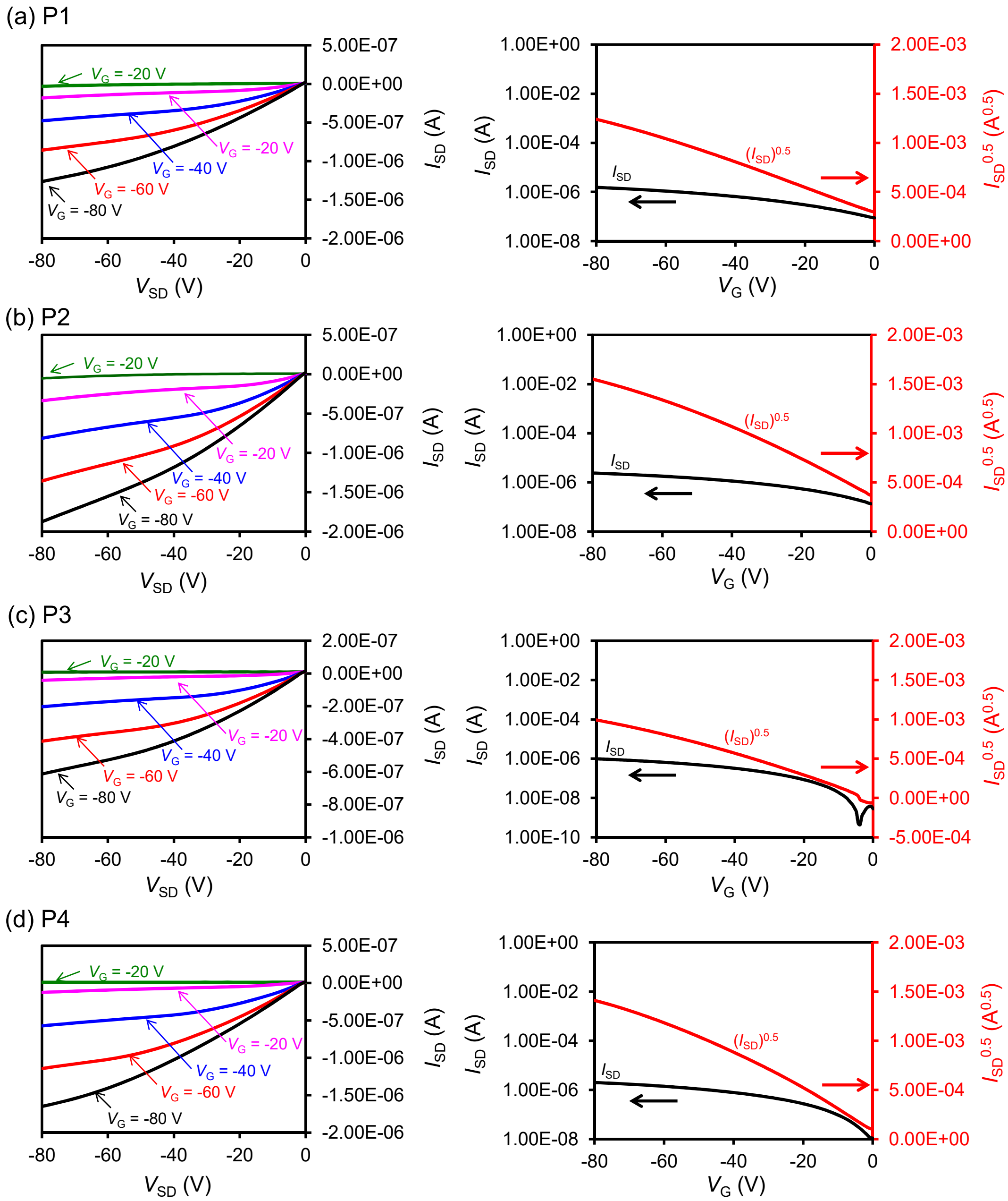

Fig. S6 Output characteristics of OFET devices.

The hole mobility of polymers was evaluated using Ossilia FACT software with saturated region.

3. Optical characteristics

3.1 Observation of optical transparency.

The overall 25 mg mixture of photoconductive polymer (70%) and FDCST (30%) was prepared in a 3-mL sample vial with 325 μL chlorobenzene. This solution was then homogeneously mixed by a rotary mixer for exactly 8 hours. After 8 hours of mixing, the polymer solution was dropped onto the ethanol pre-cleaned Teflon tape upon the glass plate. The polymer solution was then gradually dried at 80 °C in vacuum for 13 hours to obtain the polymer-FDCST composite film sheet.

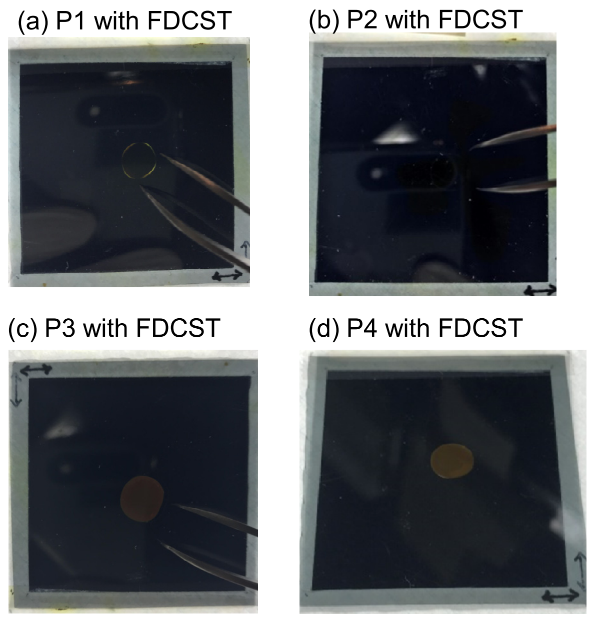

Fig. S7 Observation of optical transparency.

Table S1. Compatibility test of several chromophores.

	FDCST (20/30/40 wt%)	7-DCST (20/30/40 wt%)	AODCST (20/30/40 wt%)
P1	Δ/O/-	O/O/-	O/O/-
P2	O/O/X	X/X/-	X/X/-
P3	X/X/X	X/X/X	X/X/X
P4	X/X/X	X/X/X	X/X/X

O: good optical transparency under crossed polarizer. X: recrystallization after drying the sheet. Δ: Poor reproducibility.

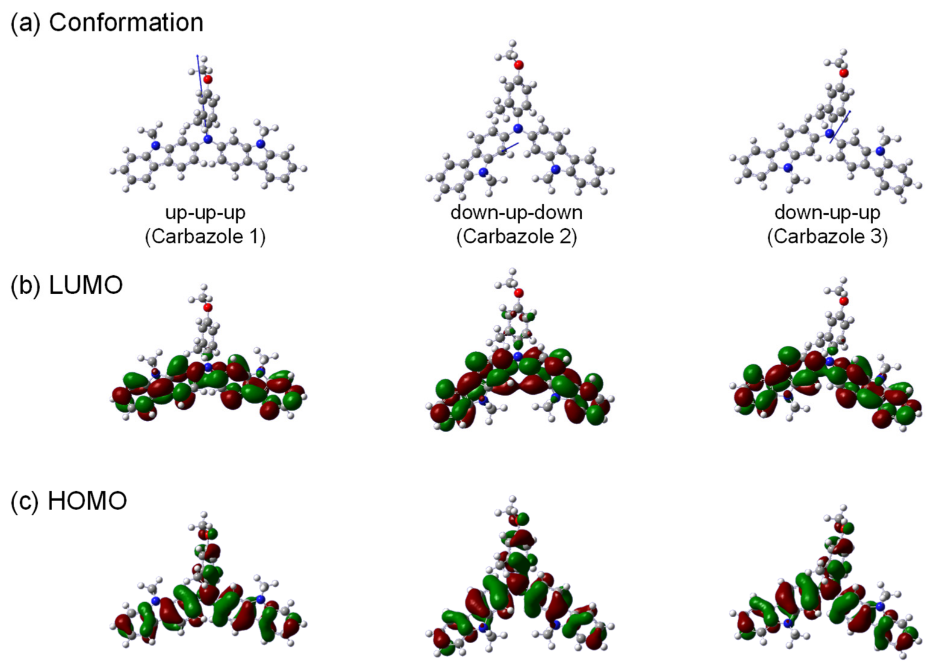

Fig. S8 Simulated molecular configuration and orbitals of simplified carbazole model.

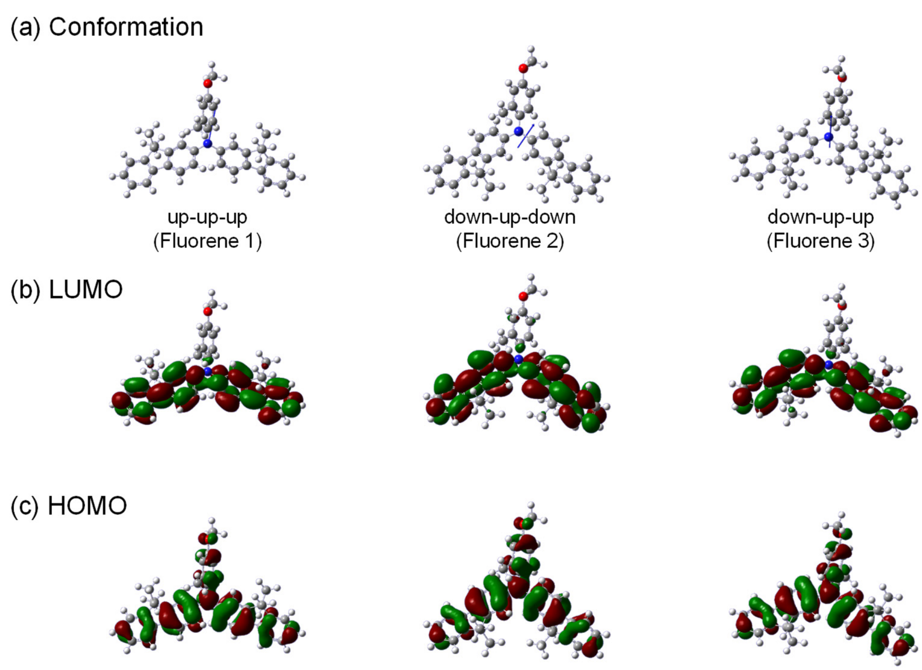

Fig. S9 Simulated molecular configuration and orbitals of simplified fluorene model.

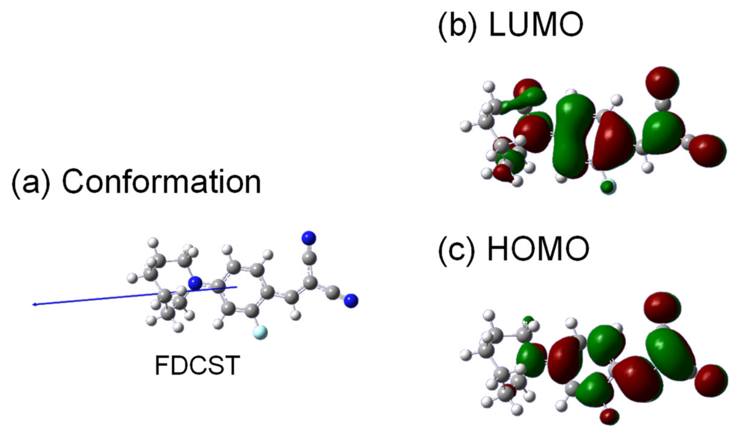

Fig. S10 Simulated molecular configuration and orbitals of FDCST.

Table S2 Calculation result of simplified molecular models with different configurations.

Model	Conformation	Dipole (Debye)	HOMO (eV)	Energy (kcal mol^{-1})
Carbazole 1	up-up-up	4.26	-4.574	-974273.173
Carbazole 2	down-up- down	1.23	-4.584	-974273.001
Carbazole 3	down-up-up	3.48	-4.571	-974273.044
Fluorene 4	up-up-up	2.26	-4.648	-1003476.475
Fluorene 5	down-up- down	1.54	-4.652	-1003476.477
Fluorene 6	down-up-up	2.07	-4.650	-1003476.447
FDCST	-	11.2	-	-727.337

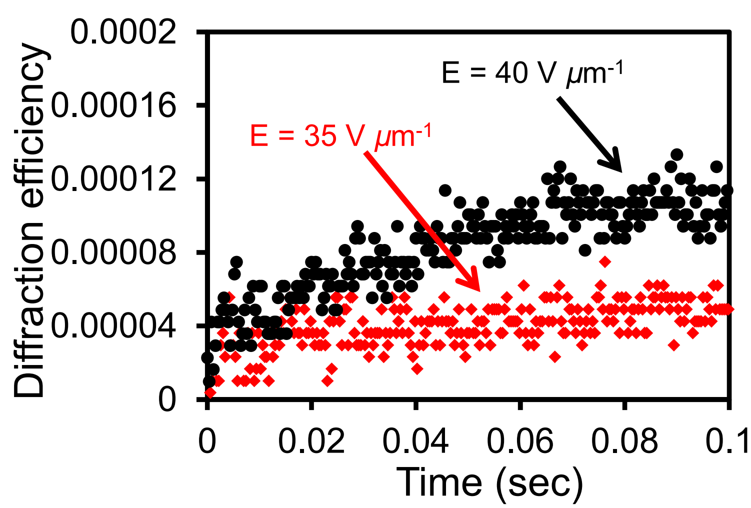

Fig. S11 PR device performance of composite of **P1**(69)/FDCST(30)/PCBM(1) with device thickness 45µm.

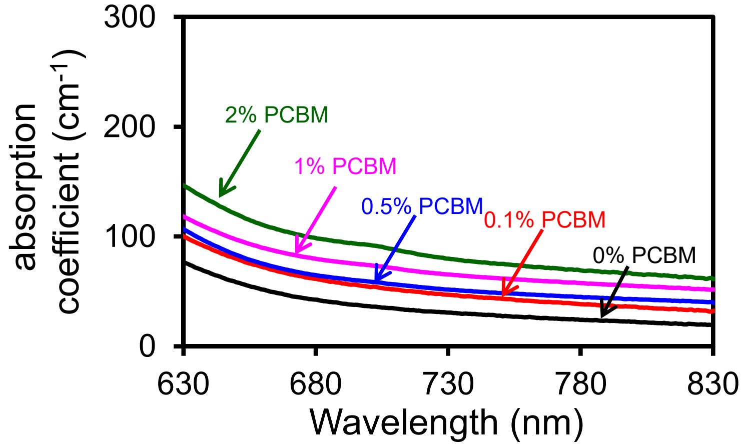

Fig. S12 UV-Vis spectra of thin film of PR composites in different loading of PCBM with **P2**. The thickness of films was controlled in a range of 25 μm and 35 μm.

Table S3 Summary of PR performances.

PR Material [a]	Laser Power (mW cm^{-2})	E_{ext} (V μm^{-1})	α_{abs} (cm^{-1})	Δn [b] (× 10^{-3})	τ (ms)	S [c] (cm^3 kJ^{-1})
P2/FDCST/PCBM (69/30/1) [d]	149 [e]	45	115	0.53	1.98	15.8
P2/FDCST/PCBM (69/30/1) [d]	642 [e]	45	115	0.70	1.47	6.4
PVK/FDCST/EHCz/PCBM (49/30/20/1) [d]	642 [e]	45	22	1.60 [d]	344	0.3
DMTPD/7-DCST/PVK/QPbS/C_{60} (44.8/44.8/9.96/0.223/0.199) [S1]	19480 [e]	100 (50)	8.04	2.02 [f] (1.66) [f]	0.4 (158)	35.2 (0.07)
PTPA-*g*-PEA/DEADCST/TNF (90/9/1) [S2]	130 [e]	50	19	0.30 [f]	8.0	15.2
PATPD/7-DCST/ECZ/C60 (49.5/35/15/0.5) [S3]	1100 [e]	71	18	1.86 [f]	8.0	11.8
Poly-TPD/P-IP-DC/BBP/PCBM (54/30/15/1) [S4]	1500 [e]	50	19	2.10 [b]	334	6.49
PTAA/PDCST/TAA/PCBM (44.5/35/20/0.5) [S5]	1500 [e]	45	48	1.00 [f, g]	1.92	2.78
$Bi_{12}SiO_{20}$ [S6]	1000 [h]	10 kV cm^{-1}	1.4 [S7]	0.016	1.6	17.8
$Sn_2P_2S_6$ [S8]	1000 [e]	0	1.0	5.00	2.50	20.0
$Sn_2P_2S_6$ [S9]	1000 [i]	0	0.4	4.00	7.00	14.3

[a] Abbreviation of materials, FDCST: fluorinated dicyanostyrene 4-homo-piperidino benzylidine malononitrile; PCBM: photosensitizer of [6,6]-phenyl C_{61} butyric acid methyl ester; PVK: poly(9-vinylcarbazole); EHCz: 9-(2-ethylhexyl)carbazole; DMTPD: *N*,*N*-Bis(3-methylphenyl)-*N*,*N*- bis(phenyl)benzidine; 7-DCST: 2-[[4-(Hexahydro-1*H*-azepin-1-yl)phenyl]methylene] propanedinitrile; QPbS: quantum dots of lead sulfide; C_{60}: fullerene; PTAA-*g*-PEA: poly(triphenylamine)-*graft*-poly(ethyl acrylate); DEADCST: 4-*N*,*N*-diethylamino-*b*,*b*-dicyanostyrene; TNF: 2,4,7-trinitro-9-fluorenone; PATPD: poly(acrylic tetraphenyldiaminobiphenol); ECZ: 9-ethylcarbazole; poly-TPD: poly(*N*,*N*-di-toly-*N*,*N*'-diphenylbiphenyldiamine); P-IP-DC: 2-{3-[(*E*)-2-(piperidino)-1-ethenyl]-5,5-dimethyl-2-cyclohexenylidene}-malononitrile; BBP: butyl benzyl phthalate; PDCST: 2-[[4-(1-piperidinyl)phenyl]methylene]propanedinitrile.

[b] Δn was calculated by the equation $\eta_0 = \sin^2 [\pi\ d\ \Delta n/\ \lambda_{prob} \cos(\alpha)]$ with using reported values, using reported values in the references for comparison.

[c] $S = \Delta n/(I_p\ \alpha_{abs}\ \tau)$, using reported values in the references for comparison.

[d] the result was obtained from this work

[e] the measurement was conducted at pumping laser of wavelength 633 nm

[f] Δn was calculated by the equation $\eta_0 = \sin^2 [\pi\ d\ \Delta n/\ \lambda_{prob} \cos(\alpha)]$. In particular, cos($\alpha$) was re-estimated from the reported geometry with assuming the refractive index of polymer composite to be 1.7.

[g] the devices thickness was re-estimated to be 75 μm.

[h] the measurement was conducted within pumping laser at wavelength 514 nm

[i] the measurement was conducted within pumping laser at wavelength 780 nm

Table S4 The energy gap between work function of ITO and HOMO level of the polymers

Material	HOMO level (or work function) (eV)	Energy bias from ITO (eV)
P1	-4.98	0.18
P2	-4.85	0.05
P3	-5.09	0.29
P4	-5.04	0.24
ITO	-4.80	-

References

S1. J.-S. Moon, T.E. Stevens, T.C. Monson, D.L. Huber, S.-H. Jin, J.-W. Oh, and J.G. Winiarz, Sub-millisecond response time in a photorefractive composite operating under CW conditions, *Sci. Rep.*, 2016, **6,** 30810.

S2. Z. Cao, Y. Abe, T. Nagahama, K. Tsuchiya, and K. Ogino, Synthesis and characterization of polytriphenylamine based graft polymers for photorefractive application, *Polymer*, 2013, **54,** 269-276.

S3. J. Thomas, C. Fuentes-Hernandez, M. Yamamoto, K. Cammack, K. Matsumoto, G.A. Walker, S. Barlow, B. Kippelen, G. Meredith, and S.R. Marder, Bistriarylamine Polymer-Based Composites for Photorefractive Applications, *Adv. Mater.*, 2004, **16,** 2032-2036.

S4. I.K. Moon, J. Choi, and N. Kim, High-performance photorefractive composite based on non-conjugated main-chain, hole-transporting polymer, *Macromol. Chem. Phys.*, 2013, **214,** 478-485.

S5. N. Tsutsumi, K. Kinashi, K. Masumura, and K. Kono, Photorefractive performance of poly (triarylamine)-Based polymer composites: An approach from the photoconductive properties, *J. Polym. Sci., Part B: Polym. Phys.*, 2015, **53,** 502-508.

S6. G.C. Valley and M.B. Klein, Optimal properties of photorefractive materials for optical data processing, *Opt. Eng.*, 1983, **22,** 226704.

S7. P. Delaye, J. C-Jonathan, G. Pauliat, and G. Roosen, Photorefractive materials: specifications relevant to applications, *Pure Appl. Opt.*, 1996, **5,** 541.

S8. A. A. Grabar, M. Jazbinsek, A. N. Shumelyuk, Y. M. Vysochanskii, G. Montemezzani, and P. Gunter, in *Photorefractive Materials and Their Applications 2: Materials*, ed. P. Günter and J-P. Huignard, Springer, New York, 1st edn, 2006, ch. 10, pp 327−362.

S9. Y. Liu, P. Lai, C. Ma, X. Xu, A.A. Grabar, and L.V. Wang, Optical focusing deep inside dynamic scattering media with near-infrared time-reversed ultrasonically encoded (TRUE) light, *Nat. Commun.*, 2015, **6,** 1-9.